Intrinsic fluorescence spectroscopy of glutamate dehydrogenase: Integrated behavior and deconvolution analysis

P. P. Pompa, R. Cingolani, and R. Rinaldi
National Nanotechnology Laboratories of INFM, Biomolecular Electronics Division, Department of Innovation Engineering, University of Lecce, Via per Arnesano 73100 Lecce, Italy
(Received 5 March 2003; published 18 July 2003)

In this paper, we present a deconvolution method aimed at spectrally resolving the broad fluorescence spectra of proteins, namely, of the enzyme bovine liver glutamate dehydrogenase (GDH). The analytical procedure is based on the deconvolution of the emission spectra into three distinct Gaussian fluorescing bands G_j. The relative changes of the G_j parameters are directly related to the conformational changes of the enzyme, and provide interesting information about the fluorescence dynamics of the individual emitting contributions. Our deconvolution method results in an excellent fitting of all the spectra obtained with GDH in a number of experimental conditions (various conformational states of the protein) and describes very well the dynamics of a variety of phenomena, such as the dependence of hexamers association on protein concentration, the dynamics of thermal denaturation, and the interaction process between the enzyme and external quenchers. The investigation was carried out by means of different optical experiments, i.e., native enzyme fluorescence, thermal-induced unfolding, and fluorescence quenching studies, utilizing both the analysis of the ''average'' behavior of the enzyme and the proposed deconvolution approach.

DOI: 10.1103/PhysRevE.68.011907 PACS number(s): 87.64.Ni, 36.20.−r, 87.14.Ee

I. INTRODUCTION

Intrinsic fluorescence spectroscopy is widely used to investigate the structural features and the behavior of proteins. The aromatic amino-acid tryptophan (Trp) provides an intrinsic fluorescent probe for protein conformation, dynamics, and intermolecular interactions. The emission spectrum is an important indicator of the integrity of the protein globular fold, as the fluorescence parameters of tryptophan residues are highly sensitive to the microenvironment of fluorophores in protein structures [1–6]. For this reason, photoluminescence has been extensively used to study a significant range of physicochemical properties of protein molecules [4,7].

Nevertheless, almost all proteins are characterized by featureless and broad emission spectra, generally originated by the ^1L_a transition [3], which limits substantially the information achievable from the analysis of integrated fluorescence spectra (which may consist of more than one component). For these reasons, different analytical approaches have been proposed in the past, aimed at spectrally resolving the broad luminescence arising from the heterogeneously emitting Trp residues, with particular efforts devoted to the determination of well defined discrete classes of tryptophans emitting at different wavelengths [5,8–10]. In the excellent works of Burstein and co-workers, the problem of the multicomponent nature of protein spectra was faced by a method based on the decomposition of tryptophan fluorescence into elementary components. In particular, the experimental spectra were interpreted as the convolution of log-normal functions (up to three terms). Each log-normal function was associated to the emission band of the single tryptophan residue in proteins: such a technique leads to the development of a model based on five statistically most probable fluorescing classes of Trps.

This analytical method well describes the experimental spectra of a large number of proteins in various structural states [5]. However, it is interesting to observe that this approach has some limitations in deconvolving the protein luminescence in the case of ''red'' spectra: native proteins with a red emission ($\lambda_{max}>342-344$ nm) or denatured proteins characterized by a large red shift ($\lambda_{max}\sim350$ nm). In this situation, in fact, the decomposition into elementary components is obtained by using a number of fluorescing classes which is always lower than the Trps actually present in the proteins, owing to the fact that the same deconvolution procedure by means of more components (i.e., three functions), with a good fit quality, does necessarily result in a Trp class with a wavelength of emission maximum quite higher than 360 nm. Such a finding is not easy to understand, although someone might observe that the physical behavior of a Trp residue in a protein (in the native or in a completely unfolded state) cannot be strictly related to that of a single and isolated Trp molecule, as the *internal* Stark effect responsible for the shifts of λ_{max} is due to the electric field imposed by the solvent but also by the protein [3,6]. Nevertheless, in the paper of Reshetnyak and Burstein [5] there are some significant cases in which an adequate deconvolution of red spectra is difficult; some examples present in that study are (we utilize the same abbreviations reported there) for native proteins, CDS—five Trps-deconvolved by one component (comp.); PLC—9 Trps-one or two comp.; BPN—3 Trps-one comp; and, for denatured, ACR.F.UR—4 Trps-one comp.; ACM.UR—24 Trps-two comp.; CHG.UR—8 Trps-one comp.; MSS.UR—20 Trps-two comp.; PAO.GDN—3 Trps-one comp.; VIN.UR—10 Trps-two comp. Hence, since the deconvolved components should directly represent the Trp classes in the proteins, such a limitation seems to be relevant. In addition, all the one-component deconvolutions do not represent a method of deeper investigation of protein dynamics, as they are completely equivalent to the analysis of the integrated behavior. Therefore, this approach represents an outstanding strategy for the determination of discrete emit-

ting classes of Trp, but has to be improved to overcome such restrictions to analyze unfolding processes, the structural features of denaturated protein, and intermolecular interactions.

In this paper, we present an alternative method to spectrally resolve protein fluorescence spectra, which seems to describe very well either red native proteins, and the complex molecular dynamics involved in the thermal- or chemical-induced protein unfolding and in the quenching processes. Here, our deconvolution method is applied to the enzyme bovine liver glutamate dehydrogenase (GDH), which seems to be appropriate for such a test. The GDH contains all three aromatic amino acids [11] but its fluorescence is dominated by the contribution of the tryptophan residues [12]. However, since GDH contains three Trp per subunit, the analysis of the integrated photoluminescence spectra is not very easy.

The analytical procedure proposed here is based on the deconvolution of the broad emission spectra of GDH, in various structural states, by means of three Gaussians (G_1, G_2, and G_3), representing the distinct contributions of the individual fluorescing species. The so-defined emitting bands are not rigorously identified with the different tryptophan residues actually present in the proteins, i.e., our fluorescing bands are not real Trp classes, as in the method previously discussed. Nevertheless, according to the photophysical characteristics of Trp, such bands are somewhat related to the fluorescing species randomly distributed in the polar or nonpolar microenvironment, thus accounting for the emission from different regions of the protein. Therefore, we identify the three different contributions as the *most inner* (G_1), *inner* (G_2), and *external* (G_3) *bands*, in relationship to the spectral regions characterizing their wavelengths of emission maximum $\lambda_{\max j}$. The relative changes of the G_j parameters are obviously correlated to the conformational changes of the enzyme, thus adding further information about the fluorescence dynamics of the individual emitting contributions to that available from the study of the integrated fluorescence spectrum.

In the deconvolution process, we do not set *a priori* any kind of restrictions to the determination of the emitting bands G_j and, in particular, no constrains are preliminary fixed for the spectral position of the three maxima ($\lambda_{\max j}$). The decomposition into elementary components was only aimed at optimizing the fitting quality of the various experimental spectra, describing a specific structural state of the protein, according to the criterion of χ^2 minimization. In some cases, such a choice may lead to the fact that the wavelength of the emission maximum of the external band ($\lambda_{\max 3}$) is much longer than the expected Trp fluorescence maximum in aqueous solution (352–354 nm). The deconvolution method proposed here provides an excellent fitting of all the spectra obtained with GDH in a number of experimental conditions (various conformational states of the protein) and is capable to describe very well the dynamics of a variety of phenomena.

In this study, we have performed different optical experiments to study the properties of GDH and to deeply characterize its conformational and structural state. This investigation was carried out by means of native enzyme fluorescence, thermal-induced unfolding, and fluorescence quenching processes, utilizing both the analysis of the ''average'' behavior of GDH and the proposed deconvolution approach.

II. MATERIALS AND METHODS

A. Enzyme and chemicals

Glutamate dehydrogenase (Lot 9029-12-3, from bovine liver, EC 1.4.1.3) was purchased from Fluka (Steinheim, Germany). Sodium phosphate was obtained from Carlo Erba (Milano), potassium iodide (99.5%) from Fluka (Steinheim, Germany), and acrylamide (99%) from Sigma.

Before all experiments, the enzyme was purified by an ultrafiltration cell (Amicon Corp. Lexington, USA) with membrane YM30, under nitrogen pressure (7×10^5 Pa). The purification was carried out at 4 °C. The resulting enzyme solution shows an A_{280}/A_{260} ratio of 1.91 [13].

B. Fluorescence spectroscopy

Fluorescence spectra were recorded by a *Perkin Elmer LS 50B* spectrofluorimeter. A xenon lamp was used as the source of excitation (2 nm bandwidth) and the emitted light was observed at right angles to the excitation radiation. Photoluminescence spectra of control samples, without protein, were recorded and subtracted from the experimental samples to correct for background interference. All the emission spectra were recorded in 20 mM phosphate buffer, *p*H 7.2 at room temperature (20 °C). The optimal excitation wavelength was determined to be 292 nm, after scanning the range between 250 and 300 nm in a 3-ml cell (1-cm light path). Concerning Trp photodegradation during the acquisition time of the spectra, we found that intensity losses were negligible or less than 5% depending on the experimental conditions.

The effect of protein concentration on fluorescence emission was also investigated. This was analyzed by monitoring the fluorescence emission parameters, as a function of the enzyme concentration, of GDH (average behavior) but also of the single emitting contributions (G_j bands) to the total broadband spectrum.

The deconvolution of the various photoluminescence spectra by the G_j bands was aimed at achieving a high-quality fitting (χ^2 criterion), without imposing any preliminary constrains. According to this analysis, the three contributions in the native state resulted in three different fluorescing bands with their maxima ($\lambda_{\max j}$) at 313.5 nm (*most inner band* G_1), 336.3 nm (*inner band* G_2), and 356.8 nm (*external band* G_3), respectively. Each G_j component exhibits a peculiar dependence of its parameters, i.e., integrated intensity A_j, linewidth w_j, and emission maximum $\lambda_{\max j}$, on the enzyme concentration, thermal treatment time and quenchers concentration, which provides information about the fluorescence dynamics of the various emitting contributions.

A very strong red shift of the external band G_3 ($\lambda_{\max 3}$ up to 410 nm) was observed, e.g., during the thermal-induced unfolding experiments. Although the occurrence of such long wavelength emission is difficult to understand, the results coming from the deconvolution analysis describe very well

the denaturation processes, perfectly integrating the assumptions derived from the investigations of the integrated behavior. The broad, red-shifted spectrum exhibited by denatured GDH is not a particular case but it is a very common feature of unfolded proteins; hence, we believe that our findings should have a more general character. In addition, it is remarkable that the deconvolution of these luminescence spectra by three bands (maintaining a reasonable fitting quality) does not admit other adequate solutions. Any attempt to fit these spectra by three Trp-like emitting species (e.g., three fluorescing species with the restriction 308 nm$<\lambda_{\max j}<$354 nm) completely fails, since the problem is not resoluble with an appropriate broadening of the external band. Furthermore, the deconvolution by four (or more) bands is an arbitrary over fitting the curves and does not provide any additional information, while the analysis with two bands does not result in an adequate fitting quality of the experimental spectra.

C. Thermal denaturation

We have characterized the structural changes of the enzyme GDH upon thermal denaturation by means of intrinsic fluorescence emission. The 3-ml samples of GDH (0.125 mg/ml) in phosphate buffer were heated in water baths at 100 °C for different times (incubation times). Aliquots were removed periodically and rapidly cooled to stop the reaction by immersion in an ice-water bath.

The denaturation process was analyzed both by monitoring the shift of the peak wavelength ($\lambda_{\max}$) of the emission spectrum as a function of the treatment time and by the shifts of the three maxima ($\lambda_{\max j}$) of the G_j bands obtained by the deconvolution, allowing us to study the contributions of the individual emitting bands to the total red-shifting spectrum.

In addition, the GDH unfolding was probed by examining the fluorescence intensity at the excitation wavelength (elastic scattering) and the thermal-induced variations of the integrated fluorescence of the enzyme (calculated as the area under the emission curves).

D. Fluorescence quenching studies

The environment of tryptophyl residues of GDH was further characterized by determining their degree of accessibility to external quenchers, acrylamide, and KI. The effect of I^- ions $[(0-0.5)M]$ and acrylamide $[(0-0.2)M]$ on the emission of GDH was tested both in native and in partially denatured conditions (1 min at 100 °C) of the enzyme (0.125 mg/ml).

The initial fluorescence F_0 of the solution (20-mM phosphate buffer, *p*H 7.2) was measured. The enzyme fluorescence from the tryptophan residues was then quenched by progressive addition of small aliquots of the stock solution of the quenchers to the fluorimetric cuvette and the fluorescence intensity F was measured again. After correction for filters effect arising from light absorption by KI and acrylamide, the decrease of fluorescence was analyzed according to the Stern-Volmer and Lehrer equations [4,14–16].

It is important to mention that information obtained by the Lehrer equation is barely qualitative, since GDH does not properly match the initial hypothesis assumed by Lehrer in his original derivation, i.e., the presence of two classes of tryptophans, one accessible and another totally inaccessible to the quencher. For this reason, in order to have a more quantitative interpretation of these experiments, the fluorescence quenching data were also deconvolved according to the procedure previously described. This allowed us to monitor the behavior of GDH in the presence of external quenchers and to evaluate the decrease in fluorescence quantum yield of the individual emitting bands, thus actually describing the mechanism of interaction between the enzyme and the quencher.

E. Statistics

For statistical considerations, the experimental results are the average of five independent measurements. The data shown in the figures throughout the paper are the mean values obtained from the experimental data, and the error bars indicate the standard deviations.

III. RESULTS AND DISCUSSION

A. Native state fluorescence

The peak intensity $I_{\max}$, the wavelength of the emission maximum $\lambda_{\max}$, and the integrated emission intensity, characterizing the photoluminescence of GDH, were measured as a function of the excitation wavelength λ_{exc}, from 250 to 300 nm, resulting in a large variation of fluorescence quantum yield, with a distinct maximum at 292 nm [Fig. 1(a)], but no change in the emission line shape [inset of Fig. 1(a)]. This suggests that only tryptophyl residues did significantly contribute to the fluorescence emission of GDH [17]. Excitation into higher states has been found to yield less fluorescence owing to nonradiative decays and quenching processes by neighboring amino acids. These findings are consistent with the results of previous papers [18]. The 292-nm radiation was chosen as the exciting wavelength in all our experiments, in order to work with the maximum quantum yield.

The fluorescence spectrum of the native GDH in phosphate buffer at *p*H 7.2, upon excitation at 292 nm, exhibits a broadband with a maximum emission $\lambda_{\max}$ at 340.5 nm. Such a $\lambda_{\max}$ value shows that the aromatic residues responsible for the fluorescence emission of GDH are located in a rather polar environment. Each chromophore is characterized by a particular microenvironment that strongly affects its emission parameters. As a consequence, the protein fluorescence results from the convolution of fluorescent contributions from individual tryptophan residues, which may vary over a rather wide range [8]. Figure 1(b) illustrates the deconvolution procedure used in this study: the broad emission spectra of GDH is deconvolved by means of three Gaussians, representing, as previously discussed, the most inner (G_1), inner (G_2), and external (G_3) fluorescing bands.

We have also investigated the dependence of fluorescence emission on protein concentration. As a general rule, low protein concentrations are commonly used in all experiments to avoid the formation of linear aggregates. In order to characterize such effects in the case of bovine liver GDH, we

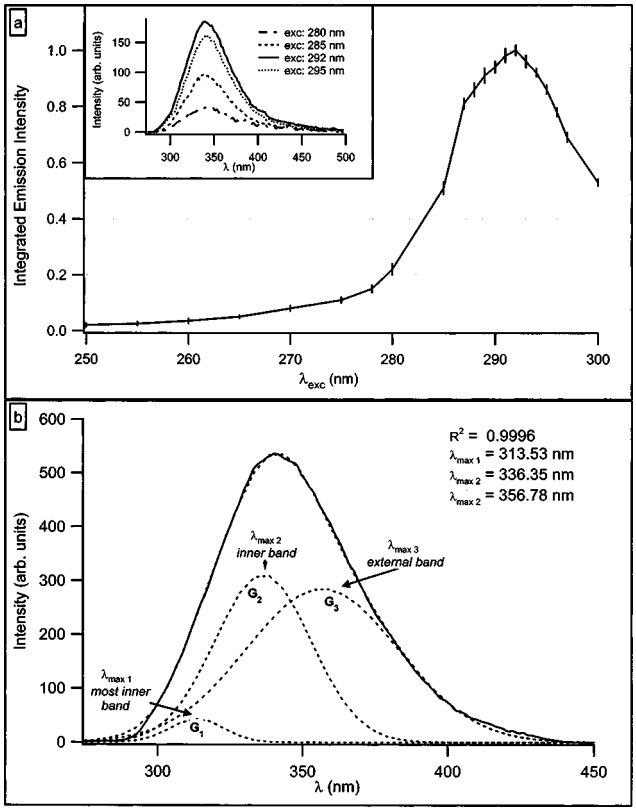

FIG. 1. Native GDH (0.125 mg/ml) photoluminescence in phosphate buffer (20 mM, *p*H 7.2): (a) relative fluorescence quantum yield (normalized to the maximum); integrated emission (calculated as the area under the curves) vs excitation wavelength; inset, examples of GDH spectra at different excitation wavelengths; (b) deconvolution analysis of the native state.

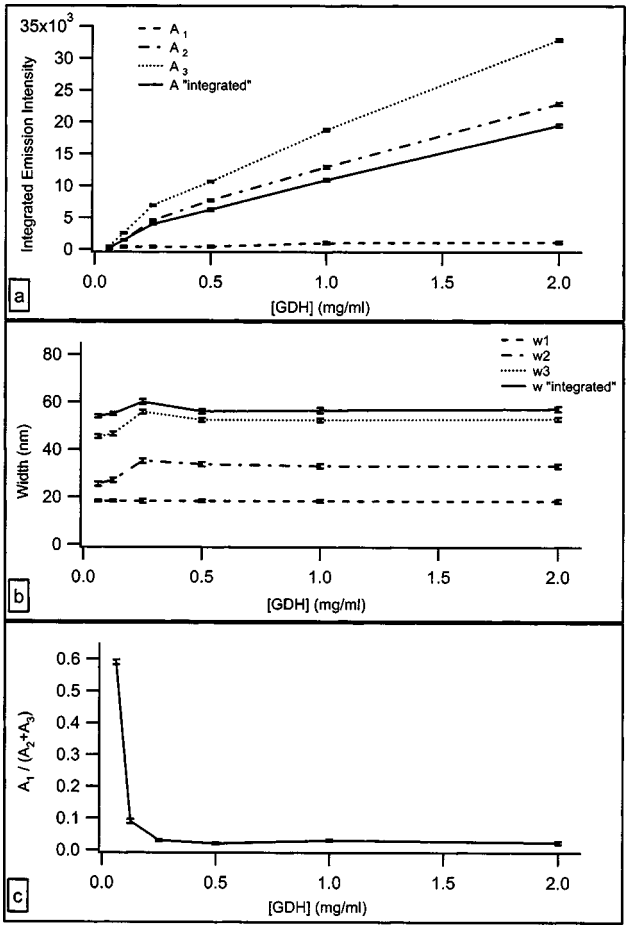

FIG. 2. Effects of protein concentration on GDH fluorescence. Analysis of the ''average'' behavior and of deconvolved bands: (a) integrated emission (divided by 3) and individual bands (arbitrary units); (b) spectral widths of the enzyme and of the three emitting bands; (c) ratio between the internal (A_1) and the external (A_2+A_3) bands vs protein concentration.

analyzed both the integrated enzyme photoluminescence (the average emission) and the three G_j bands as a function of protein concentration.

As shown in Fig. 2(a) (continuous line), a clear change of slope occurs (at 0.25 mg/ml) in the curve describing the integrated emission of GDH versus protein concentration. In the examined range of concentrations, such dependence may be represented by two different linear regions, suggesting the presence of two marked behaviors in the fluorescing process. This experimental evidence is in agreement with previous studies on GDH, in which protein concentrations always lower than this value (0.25 mg/ml) were utilized [19,20]. The lowest molecular weight form of the bovine liver GDH, which is enzymatically active and stable in aqueous solution, consists of a hexamer of identical folded peptide chains each having a molecular weight of about 56 000 [11,21]. The hexamer is also the lowest molecular weight form for which catalytic activity can be demonstrated. In more detail, as reported by Fisher [13], the enzyme is completely in the form of hexamer, at protein concentrations below 0.1 mg/ml, whereas, with increasing protein concentration, the hexamers may associate, thus affecting the optical properties of the biological system. In this case, the linear dependence of the fluorescence intensity on the concentration is lost. On the other hand, it is widely recognized that the specific reaction rate of the enzyme is independent of the protein concentration and the catalytically active sites themselves are quite unaffected by the possible associations of hexamers [13].

The photoluminescence characteristics of the integrated GDH (spectral width and integrated emission) have been compared with the corresponding variations of the G_j components of the spectrum. Despite the average analysis would suggest a sort of ''two-state'' behavior, at least in the examined range of protein concentrations, a careful interpretation of deconvolution data demonstrates a more composite process, in which the three single contributions are differently affected by protein-protein interactions.

The variations of the spectral widths with increasing enzyme concentration are reported in Fig. 2(b). As shown, either the average curve and the G_j bands are weakly influenced by the GDH concentration and are virtually constant in the whole range. On the other hand, as displayed in Fig. 2(a), the G_j emission yields are quite different, due to the possible enhancement of hexamers association. The two ''outer'' bands (G_2 and G_3) show a similar behavior, also comparable to the average curve, but the increase in the emission

efficiency is quite faster than the protein molecule as a whole, especially for the external band G_3. On the contrary, the most inner band G_1 shows a completely different trend, resulting almost unaffected by the GDH concentration. Such a discrepancy is evidenced in Fig. 2(c), where the ''internal'' emission is directly related to the external contributions. This analysis unambiguously demonstrates the diverse influence of the different ranges of protein concentration on the individual fluorescing bands, revealing that a ratio approximately constant is observed only at concentrations higher than 0.25 mg/ml, whereas large variations in the emission yield of the distinct fluorescing bands occur in the first part of the curve.

This point deserves further comment. First, the most inner fluorescing band G_1 (λ_{max} at 313.5 nm) increases quite slowly with increasing enzyme concentration, suggesting a potential fluorescence quenching effect, somewhat due to the hexamers association. This experimental evidence might lead to speculations about possible variations in the folding properties of the enzyme, induced by the higher extent of subunits association. Second, the change in the slope of the whole GDH molecule (at 0.25 mg/ml) is essentially caused by the two external bands (G_2 and G_3). This process may disclose the existence of a critical level of hexamers association that is capable to strongly affect the outer fluorescing states.

In addition, it is interesting to point out that, despite the apparent two-state behavior of the average enzyme, the ratio of the internal emission to the external ones [Fig. 2(c)] reveals the occurrence of a more complex trend than a simple two-state phenomenon.

B. Thermal denaturation

As reported by Fisher [13], the enzyme has an unusually high degree of thermal stability relative to that of other dehydrogenases and to those of most other proteins found in the liver. We have characterized the structural changes of GDH upon thermal denaturation by measuring the changes of the intrinsic fluorescence spectra. This process may be reversible or irreversible [22]. Thermal treatment affects the protein structure by exposing hydrophobic residues which were otherwise shielded in the core of the protein in its native state. The change in the optical response of the enzyme may thus be used to monitor the externally induced alterations on the protein folding leading to the exposure of some amino-acids residues and to the shielding of others.

Figure 3(a) represents the fluorescence spectra, obtained upon standard conditions, of GDH subjected to a range of thermal treatment (0–15 min at 100 °C). As shown, the denaturation process evidently results in a red shift of λ_{max}, followed by a decrease in intensity at λ_{max} and an increase of linewidth.

The shift of λ_{max}, induced by the thermal treatment at 100 °C, is analyzed in Fig. 3(b). The incubation times range from 0 to 15 min. The maximum emission of the tryptophan residues is slightly red shifted from 340.5 to 344.5 nm. Since the fluorescence of tryptophan residues primarily depends on their local environment, this alteration in the emission spectra indicates that the aromatic residues buried within the hydrophobic core of the native protein have been exposed to the aqueous solvent during unfolding [23]. This indicates that, after a high-temperature treatment, the structure around the chromophores has a more pronounced hydrophilic character than in the native state. However, the λ_{max} values are weakly affected by such a structural change. The maximum shift observed (344.5 nm) is slightly smaller than the value of 352–354 nm, expected for tryptophyl side chains in a completely unfolded polypeptide chain. It may be also significant that, in these experimental conditions, the thermal unfolding of bovine liver GDH appears as a rather gradual process. The red-shift curve steadily increases in the denaturation range, suggesting the occurrence of a more complex trend than a simple two-state transition.

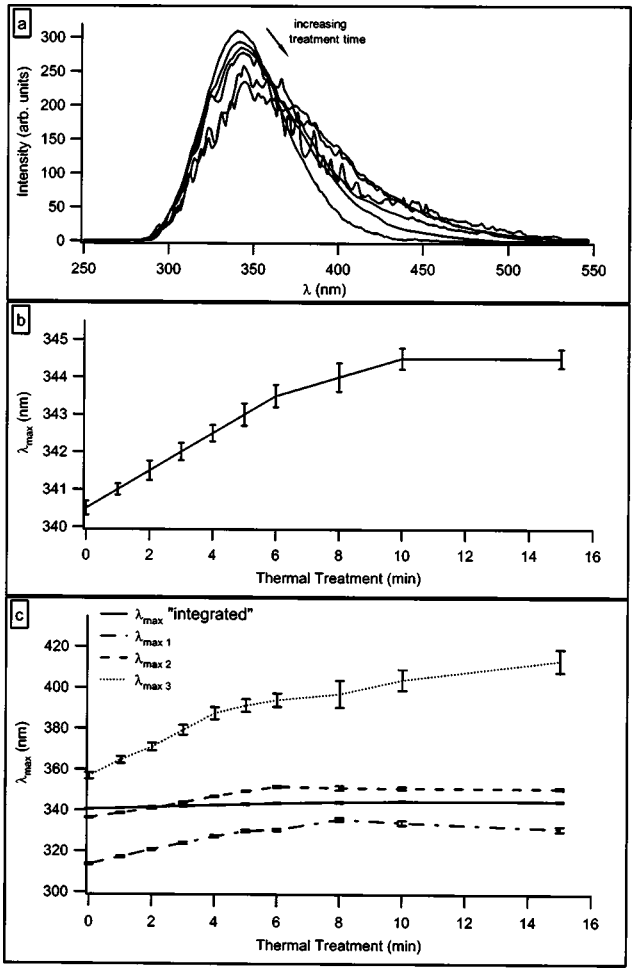

FIG. 3. Thermal denaturation: (a) Fluorescence spectra of GDH subjected to a range of thermal treatment (0–15 min at 100 °C); (b) shift of λ_{max} as a function of the treatment time; (c) deconvolution analysis, shift of λ_{max} of the three emitting bands and comparison with the average behavior.

A deeper insight in the denaturation process is obtained by analyzing the behavior of λ_{max} of the G_j bands constituting the fluorescence spectrum [Fig. 3(c)]. While the average λ_{max} would suggest a slow but regular denaturation process in which the internal tryptophans possibly experience solvent exposure, the G_j dependence suggests a more complicated model, where different phenomena may account for protein

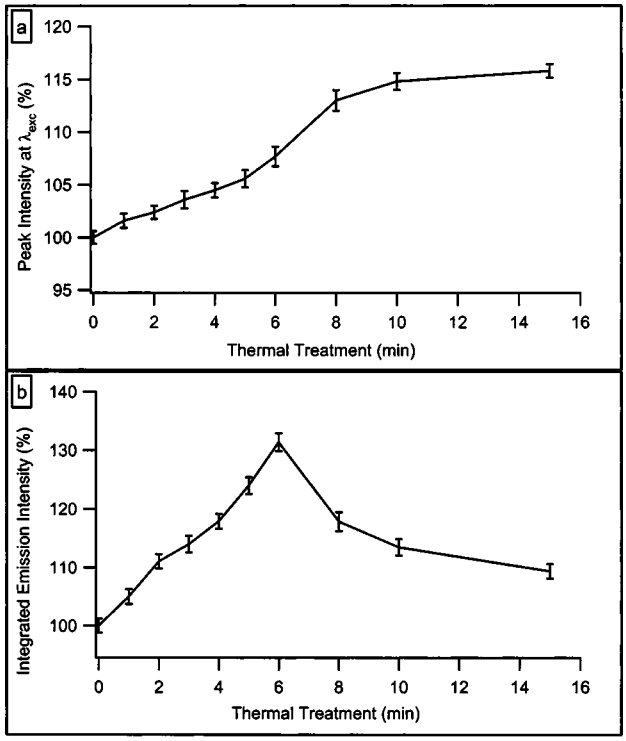

FIG. 4. Thermal denaturation: (a) intensity at λ_{exc} (elastic scattering); (b) integrated fluorescence emission (area under the curves) vs treatment time (native state is 100%).

unfolding. The two internal bands ($\lambda_{max\,1}$ and $\lambda_{max\,2}$) show a similar behavior, with a red shift occurring only in the first 6–8 min of the denaturation curves. For longer times, a blue shift trend becomes evident. On the other hand, the external band ($\lambda_{max\,3}$) shows a continuous red-shift behavior. It may be possible that, during the initial phase of the unfolding process, internal tryptophans become more exposed to the solvent, then the thermal-induced conformational changes cause aggregation processes, which may account for the inversion of the spectral shifting. In contrast, the external contribution does not seem to be affected by such aggregation phenomena. This conjecture, however, will be further discussed.

The GDH denaturation was also monitored by the relative intensity of the right angle elastic scattering [Fig. 4(a)]. This technique provides a qualitative evidence of the molecular mass increase on protein association [24]. A large enhancement of scattered light was observed after thermal treatment [Fig. 4(a)] possibly indicating that aggregation has occurred during such treatment. This association seems to be irreversible, as previously reported for GDH after pressure-induced inactivation [25]. The conformational changes suggest that protein denaturation partially result in the formation of aggregates, such behavior indicating that irreversible thermal denaturation is also due to polymolecular processes. Although the elastic scattering curve shows no breaks or discontinuities, also in this case a marked variation of the slope in the region between 6 and 8 min is evident. This clearly indicates the induction of a small temperature-dependent structural transition. On the other hand, Fig. 4(b) shows the variations of the integrated fluorescence of GDH incubated at 100 °C for different times. Such variations are consistent with the current discussion: in the first step of the unfolding process (up to 6 min), Trp residues increase their quantum yield and thus protein emission, owing to a minor quenching efficiency by neighboring amino acids; then, for longer times, the self-association effect, due to unfolded conformation, causes a large decrease in the emission intensity.

In addition, it is interesting to point out that the gradual and continuous aggregation phenomenon takes place simultaneously with the unfolding process [Fig. 4(a)]. Nevertheless, in the final part of the plot, self-association curve was characterized by a plateau, possibly indicating the existence of a maximum limit to aggregation caused by thermal denaturation.

C. Fluorescence quenching

The wavelength of maximum fluorescence intensity λ_{max} is commonly used as an indicator of exposure to water and well correlates with the efficiency of external quenchers [3]. In this regard, the class of proteins with λ_{max} at about 340 nm is extremely interesting because these are usually quite accessible to external quenchers.

Acrylamide is a polar, uncharged compound that has been shown to quench the fluorescence of indole derivatives predominantly by collisional processes [15], affecting both the exposed and masked fluorophores [26]. Interestingly, the quenching efficiency of tryptophyl residues in proteins by acrylamide is independent of the polarity of their microenvironment and depends exclusively on the collisional cross section [27]. On the other hand, the ionic quencher KI selectively quenches the emission of exposed Trps [26]. Iodide is negatively charged and therefore, it is only capable to quench surface tryptophanyl residues.

In all our experiments on GDH, we found that the fluorescence intensity decreases with increasing quencher concentration with no apparent discontinuity. In all these experiments no shift in the emission maxima was observed. The Stern-Volmer plots are reported in Figs. 5(a) and 5(b), for acrylamide and KI, respectively. As expected, the effect of iodide quenching on GDH is less pronounced in comparison with acrylamide [Figs. 5(b) and 5(a)]. The red emission maximum of the native protein (340.5 nm) suggests that the tryptophan residues of GDH are not so buried and inaccessible to the quencher. For the denatured enzyme, the fractions of fluorophore available to the quencher are higher, indicating that a conformational change has taken place, with a partial unfolding of the protein. For acrylamide [Fig. 5(a)], the Stern-Volmer plots give values for the quenching constant K_q of 11.38 and 15.24 M^{-1}, for the native and thermally treated enzyme, respectively. On the other hand, despite the negative charge in the surface of the protein, the ionic quencher KI induces non-negligible quenching effects [Fig. 5(b)], with a K_q value of 0.59 M^{-1}, for native GDH (in the thermally treated enzyme, the fit was nonlinear). The Stern-Volmer plots provide a sensitive measure of the exposure of fluorescent Trp residues. When the protein sterically

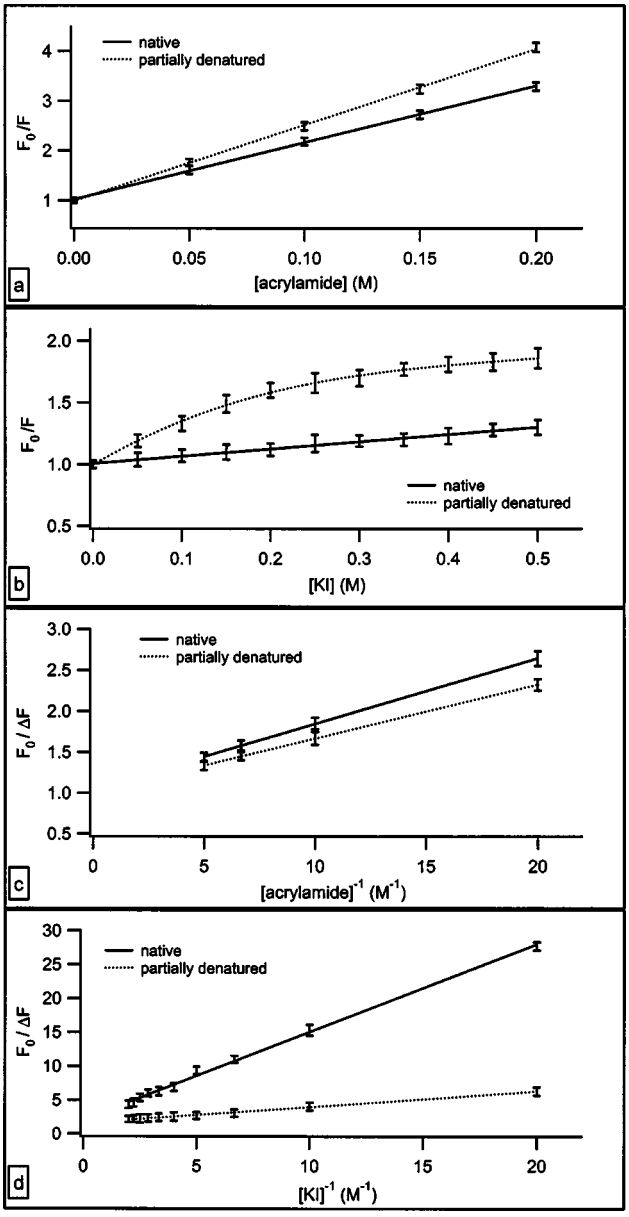

FIG. 5. Fluorescence quenching of GDH by added acrylamide (0–0.20 *M*) and KI (0–0.5 *M*): Stern-Volmer plots of acrylamide (a) and KI (b); Lehrer plots of acrylamide (c) and KI (d).

shields a Trp residue from the solvent, this will be reflected in a reduced K_q value.

The modified Stern-Volmer (Lehrer) plots are reported in Figs. 5(c) and 5(d). We observe for acrylamide a value of 96% (1/intercept) for the Trps available to the quencher in the native state, whereas in the thermally treated enzyme all tryptophan residues (99%) are found to be accessible. As expected, the corresponding values for the ionic quencher KI are lower. In fact, in this case, we found that only 48% and 61% of the fluorescing species, respectively, for the native and denatured states, are directly affected by the presence of an external quencher. However, as previously discussed, this latter analysis only provides a qualitative indication about the different efficiency of the two quenchers, since the extrapolated results do not correctly represent the physical situation of the protein. In addition, the information derived only from this kind of analysis does not account for the lack of spectral shifting, which can be potentially induced by the quenching process, particularly if charged molecules (I^-) are used. In order to properly explain these experiments, thus providing a satisfactory description of the interaction process between the enzyme and the quencher molecule, we utilized also in this circumstance the deconvolution approach (only for the native state). This allowed us to independently monitor the variations of the fluorescence parameters in the single G_j bands, therefore recognizing the extent of the interaction of the external quencher with each of them. In Fig. 6, the decrease in the fluorescence quantum yield of the single emitting bands is represented as a function of the quencher concentrations. Interestingly, the deconvolution analysis revealed that, unlike the emission yields, the single bands are not affected by the quenching mechanism with regard to the position of the three λ_{max} and the values of the spectral widths, both in the case of acrylamide and KI (data not shown). For acrylamide quenching [Fig. 6(a)], it seems that the external bands (G_2 and G_3) are more sensitive to the quencher action, with respect to the most inner one. In addition, in consideration of the experimental trends shown by the single bands, especially for the continuing and dissimilar variations in the slope of the external ones, the quenching process appears as a composite phenomenon, in which the concentration of the quencher plays a fundamental role. In-

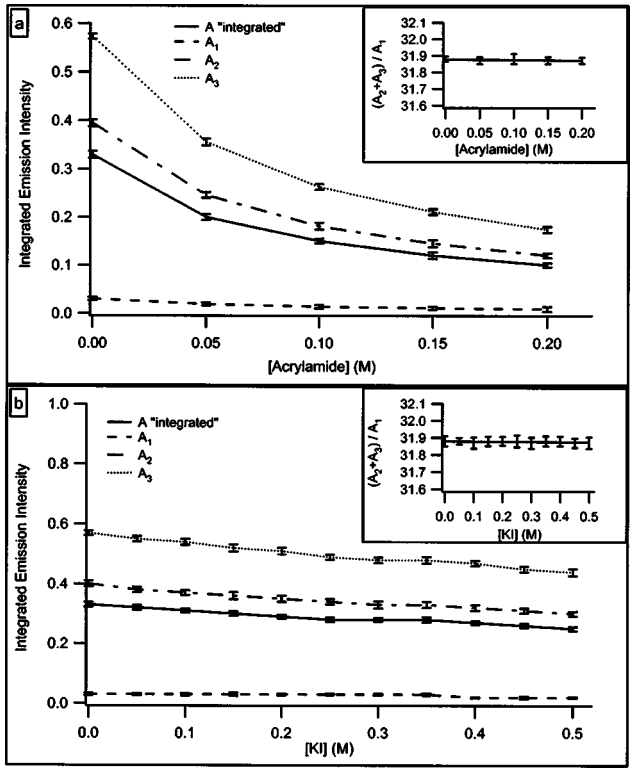

FIG. 6. Deconvolution analyses of fluorescence quenching processes. The relative contributions of the single emitting bands and the integrated GDH photoluminescence (divided by 3) are represented with increasing acrylamide (a) and KI (b) concentrations. In the insets the ratios between the external bands and the most inner one are shown vs acrylamide and KI concentrations.

deed, it seems that the different ranges of acrylamide concentration differently interact with the individual emitting bands, thus entailing an intricate dependence of the collisional cross section of the process on the quencher concentration. On the other hand, if the ratio between external and internal bands is examined [inset of Fig. 6(a)], no dependence of the efficiency of the average phenomenon on acrylamide concentration is revealed. This experimental evidence may reasonably account for the linear relationship between the decrease in fluorescence intensity and the quencher concentration [Fig. 5(a)] and for the lack of any spectral shifting in the global spectrum of the enzyme.

Analogous considerations can be made when KI is used as the external quencher [Fig. 6(b)]. Obviously, in this case, the effectiveness of the quencher action is quite lower than for acrylamide. In this case, it is possible, however, to note a more regular trend of the quenching mechanism, with no clear variations in the slopes of the experimental curves. Nevertheless, as shown in the inset of Fig. 6(b), we cannot detect a strong prevalence of the external band $A3$ quenching, as predictable owing to the intrinsic properties of an ionic quencher. This experimental finding is a little surprising and explains the absence of any spectral shifting in GDH quenching by KI. It might be possible that, since the fluorescing contribution of the most inner band G_1 is a very small fraction (about 3%) of the integrated enzyme emission, such particularly small deviations in the emission yield were not correctly detected in our experiments. However, comparable results were obtained in a previous study [16] and no spectral shifts were induced by iodide quenching. Although such occurrence was not specifically deepened by the authors, this result still remains rather remarkable, also because, as shown in Fig. 6(b), no differences in the emission trend were measurable between the external G_3 and the inner bands G_2.

IV. CONCLUSIONS

In this paper, we have characterized several aspects of the enzyme glutamate dehydrogenase by means of intrinsic fluorescence spectroscopy. Different optical experiments were performed to investigate its conformational and structural state. A deeper insight in the fluorescence dynamics was obtained by a deconvolution method of the enzyme photoluminescence spectra into three individual fluorescing bands G_j, which adds further information to that available from the study of the integrated spectrum alone. Our deconvolution approach resulted in an excellent fitting of all the spectra obtained with GDH in different experimental conditions and was capable to carefully explain various intricate phenomena. In particular, the analysis of the G_j bands allowed us to deeply characterize the dependence of hexamers association on protein concentration, the detailed dynamics of thermal-induced unfolding, as well as the absence of spectral shift in the presence of the ionic quencher KI. All these postulations were not recognizable by the examination of the average protein alone.

Concerning the puzzling results related to the red wavelength of the emission maximum $\lambda_{\max 3}$ of the external band G_3, we have shown that no preliminary constrains for the spectral position of the three maxima ($\lambda_{\max j}$) have to be imposed to obtain a suitable fitting quality of the various experimental spectra. In fact, in some cases, proteins actually fluoresce also at such longer wavelengths, though the physical meaning of the red fluorescing band G_3 is yet rather unclear.

In this study, we have utilized the deconvolution analysis to characterize a specific system (GDH), but the proposed methodology is thorough and general, and hence some of the conclusions can also be applied to other biological systems. We have shown that this approach can provide a higher understanding of the intrinsic fluorescent signals in a wide range of experimental situations, and thus, beyond the fundamental investigation of the structural features of proteins, it may be promising for a large class of biological or biophysical issues. Specifically, we believe in the general applicability of the proposed deconvolution method to many areas of the biomedical research in which intrinsic fluorescence spectroscopy is routinely used, with the advantage of providing a deeper understanding of the mechanisms underlying some biological processes, such as ligand-receptor interactions, owing to a more specific interpretation of the related conformational transitions, a possible improvement in the explanation of the complex quenching mechanisms elicited by a variety of physiological processes or a higher characterization of fluorescence spectra of different tissues (healthy or tumorous).

[1] M. R. Eftink, Methods Biochem. Anal **35**, 127 (1991).
[2] K. Doring, L. Konerman, L. Surrey, and F. Jahnig, Eur. Biophys. J. **23**, 423 (1995).
[3] P. R. Callis, Methods Enzymol. **278**, 113 (1997).
[4] J. R. Lakowicz, in *Principles of Fluorescence Spectroscopy*, 2nd ed. (Plenum Press, New York, 1999).
[5] Y. K. Reshetnyak and E. A. Burstein, Biophys. J. **81**, 1710 (2001).
[6] J. T. Vivian and P. R. Callis, Biophys. J. **80**, 2093 (2001).
[7] Y. Chen and M. D. Barkley, Biochemistry **37**, 9976 (1998).
[8] E. A. Burstein, N. S. Vedenkina, and M. M. Ikova, Photochem. Photobiol. **18**, 263 (1973).
[9] E. A. Burstein, S. M. Abornev, and Y. K. Reshetnyak, Biophys. J. **81**, 1699 (2001).
[10] Y. K. Reshetnyak, Y. Koshevnik, and E. A. Burstein, Biophys. J. **81**, 1735 (2001).
[11] K. Moon, D. Piszkiewicz, and E. L. Smith, Proc. Natl. Acad. Sci. U.S.A. **69**, 1380 (1972).
[12] C. L. Bashford, in *Spectrophotometry and Spectrofluorimetry: A Practical Approach*, edited by C. L. Bashford and D. A. Harris (IRL Press, Oxford, 1987), p. 1.
[13] H. F. Fisher, Methods Enzymol. **113**, 16 (1985).
[14] S. S. Lehrer, Biochemistry **10**, 3254 (1971).
[15] M. R. Eftink and C. A. Ghiron, Biochemistry **15**, 672 (1976).

[16] J. Ferrer, R. Cremades, C. Pire, and M. J. Bonete, J. Photochem. Photobiol., B **47**, 148 (1998).
[17] J. C. Brochon, Ph. Wahl, J.-M. Jallon, and M. Iwatsubo, Biochemistry **15**, 3259 (1976).
[18] H. B. Steen, J. Chem. Phys. **61**, 3997 (1974).
[19] E. Gabellieri Strambini and G. B. Strambini, Biosens. Bioelectron. **15**, 483 (2000).
[20] S. Ghobadi, S. Safarian, A. A. Moosavi-Movahedi, and B. Ranjbar, J. Biochem. (Tokyo) **130**, 671 (2001).
[21] M. Cassman and H. K. Schachman, Biochemistry **10**, 1015 (1971).
[22] T. J. Ahern and A. M. Klibanov, in *Methods of Biochemical Analysis*, edited by D. Glick (Wiley, New York, 1988), p. 91.
[23] F. X. Schmid, in *Protein Structure: A Practical Approach*, edited by T. E. Creighton (IRL Press, Oxford, 1989), p. 251.
[24] D. N. Teller, Methods Find Exp. Clin. Pharmacol. **2**, 277 (1971).
[25] K. Fukushima, K. Matsumoto, M. Okawauchi, T. Inoue, and R. Shimozawa, Biochim. Biophys. Acta **872**, 42 (1986).
[26] M. R. Eftink and C. A. Ghiron, Anal. Biochem. **114**, 199 (1981).
[27] S. Zerhouni, A. Amrani, M. Nijs, N. Smolders, M. Azarkan, J. Vincentelli, and Y. Looze, Biochim. Biophys. Acta **1387**, 275 (1998).